COMMUNICATIONS IN SCIENCE AND TECHNOLOGY
Homepage: cst.kipmi.or.id

Hollow mesoporous silica nanoparticles functionalized with Pluronic for controlled drug release

Ngoc Tram Nguyen Thi* and Ngoc Huyen Nguyen Thi

College of Medicine and Pharmacy, Tra Vinh University, Vinh Long Province 85000, Vietnam

Article history:
Received: 9 December 2025 / Received in revised form: 13 April 2026 / Accepted: 22 April 2026

Abstract

In recent years, innovative drug-delivery systems have been considered one of the most crucial techniques for enhancing cancer treatment. In this study, F127, a thermal-sensitive polymer, was utilized to conjugate to the surface of HMSN, and subsequently, the carriers were loaded with Dox. The obtained product was characterized by a series of experiments, including TEM, FT-IR, TGA, XRD, and zeta potential. The HMSN-F127 carrier system was successfully synthesized with a size of 152.9 ± 0.9 nm. Furthermore, the SEM results revealed that the pores were located within the material. The zeta potential was determined to be -4.03 ± 0.15 mV, with a corresponding surface area of 168.4 m^2/g. The efficiency and drug loading capacity of HMSN-F127 were found to be higher than those of naked HMSN with DLE and DLC values of 72.08 ± 0.09 % and 11.09 ± 0.01 %, respectively. In particular, Dox was well controlled by HMSN-F127. At concentrations ranging from 0 - 250 µg/ml, HMSN-F127 was not toxic to HCC J5 cells. The findings demonstrate that the HMSN-F127 system provides an effective platform for enhancing drug loading and achieving controlled drug release, thereby highlighting its potential for improved anticancer drug delivery and future development of stimuli-responsive nanocarriers.

Keywords: Drug delivery system; doxorubicin; *fluronic; hollow mesoporous silica nanoparticles;* thermosensitivity

1. Introduction

Since 2000, mesoporous silica nanoparticles (MSN) have been the subject of extensive studies in the field of biomedical applications [1]. In comparison to polymer nanoparticles, micelles and liposomes, MSN has been identified as a promising nanocarrier due to high biocompatibility, large surface area and pore volume, and easy surface modification [2,3]. Hollow mesoporous silica nanoparticles (HMSN) have recently become a subject of interest for scientists. HMSN have a capillary structure similar to MSN and internal pores, thereby enabling it to contain more drug molecules. This characteristic reduces the possibility of the accumulation of foreign materials in the body, thus promising the potential to replace MSN in the future. However, in the structure of the HMSN particle shell, there are capillary tubes that are directly connected to the internal pores, so the drug is easily leaked during transportation. The issue, therefore, lies in the coverage of these capillary pores through the modification of the surface of the HMSN particles with organic molecules or polymers. These molecules act as "caps" to cover the capillary pores to increase the drug-carrying efficiency and control drug release [2].

Pluronic (F127), approved by the FDA and listed in the US and European Pharmacopoeia, is also referred to as Poloxamer 407. It has been the focus of extensive studies and has been applied in drug delivery due to its high biocompatibility and in particular its thermosensitivity [4, 5]. The LCST (lower critical solution temperature) of F127 can be varied from 25 - 37°C by adjusting the concentration, indicating that F127 exists as chains at room temperature and aggregates at body temperature [6,7]. Based upon these advantages, F127 is a popular material for synthesizing thermosensitive nanoparticles for controlled drug release [7-9]. Recently, this poloxamer has been studied for modification on the surface of nanocarriers such as dendrimers and MSNs to enhance the rate of drug release in cancer treatment. In particular, for carrier systems with capillary structures, F127 acts as a cap to retain the drug inside the capillary pores after

* Corresponding author.
Email: tram06@tvu.edu.vn
https://doi.org/10.21924/cst.11.1.2026.1861

encapsulation and prevents rapid drug release during use [10, 11]. For example, Zhao *et al*. reported the synthesis of SBA-15 using Pluronic as a structure-directing agent, highlighting its role in forming well-ordered mesoporous silica[12]. In addition, Liu *et al*. (2009) developed silica cross-linked F127 micelles loaded with iron oxide nanoparticles, demonstrating enhanced structural stability and good dispersibility for biomedical applications [13].

Dox was approved for medical use in the United States in 1974. This medication is listed among the safest and most efficient medications required in a healthcare system by the WHO's List of Essential Medicines [14]. Dox is an effective chemotherapy agent that increases survival in cancer patients, but its use is hampered by cardiotoxicity. Cardiotoxicity, a recognized side effect of Dox, can manifest as an acute or chronic condition twenty years after treatment. This side effect is particularly significant in children treated with Dox. Other typical side effects include nausea, hair loss, gastrointestinal problems, and nervous system disturbances (often causing hallucinations and dizziness) [15,16]. To enhance the treatment effectiveness and reduce the side effects of Dox, the method of introducing drugs into nanocarrier systems to formulate targeted drug delivery systems has received a significant interest from scientists.

In this study, the successful synthesis of F127 conjugated HMSN was achieved through the reaction between aminated HMSN and activated F127. The obtained products were characterized by a series of experiments, including TEM, FT-IR, TGA, XRD, and zeta potential. Dox was encapsulated and the calculated for drug loading efficiency and capacity. *In vitro* release and cell viability tests were also examined to evaluate the advantages of HMSN-F127. The objective of this study is to elucidate the role of stable F127 association in modulating the drug loading and release behavior of HMSN-based nanocarriers.

2. Materials & method

2.1. Materials

The chemicals utilized in the study were of all analytical grade and high purity, including: Doxorubicin (Dox), Cetyltrimethylammonium bromide (CTAB), and Tetraethyl orthosilicate (TEOS) from Sigma. Furthermore, Ethanol (Prolabo), NH_3 25%, Sodium carbonate from Merck, Glacial Acetic acid from Fisher, and deionized water. Cellulose membrane MWCO 12–14 kDa (Spectrum Laboratories, Inc., Rancho Dominguez, CA 90220, USA).

2.2. Synthesis of HMSN

The synthesis of hollow mesoporous silica nanoparticles (HMSN) was accomplished through the utilization of the hard-template method. This method is well recognized in view of its capacity to control the particle formation process and particle size. The synthesis process involves 3 stages: (1) Synthesis of solid silica nano cores (SSN), (2) Coating the shell to form the core-shell structure (SSN@CTAB/SSN), and (3) Etching the core to form hollow silica nano-particles (HMSN). The synthesis process was conducted in accordance with the published research of the group [17]. Firstly, SSNs were synthesized employing the Stober method. A mixture of ethanol (13.5 M), deionized water (deH_2O) (6.0 M), and NH_3 (0.38 M) was stirred for a period of 30 minutes at a temperature of 50 °C. Subsequently, TEOS solution (0.29 M) was added to the mixture, and the reaction was carried out for a period of 6 hours. SSN was subjected to membrane dialys (MWCO 12-14 kDa) in deH_2O and was freeze-dried. Furthermore, the SSN@CTAB/SSN process was carried out through the coating of the mesoporous silica nanoshells onto the SSN particles. SSN were dispersed in deH_2O and stirred with the surfactant CTAB (0,05 M) for 30 minutes at 50°C. Thereafter, an ethanol (EtOH) solution and NH_3 were added to the mixture (1.43:0.05, M/M), and TEOS (0.27 M) was added last and the mixture was stirred for a duration of 6 hours at 50°C. The product was dialyzed with a 12-14 kDa cellulose membrane in deH_2O and lyophilized. Finally, the SSN@CTAB/SSN particles were dispersed in deionized water and stirred for 30 minutes. 0.2 M Na_2CO_3 solution, following this was added. The reaction was performed for a period of 9 hours. The obtained product was then dialyzed with a 12-14 kDa cellulose membrane in a mixture (CH_3COOH: EtOH 1:1 v/v). Following this, the product was dialyzed once more with deH_2O and freeze-dried to obtain HMSN.

2.3. Synthesis of HMSN-NH_2 and NPC-F127-OH

The surface of HMSN was modified with amine groups by co-condensation using a silica precursor containing amine groups, 3-aminopropyltriethoxysilane (APTES). A 100 mg of HMSN was dispersed into ethanol and sonicated for 15 minutes. Subsequently, a mixture of APTES and EtOH (4:1, v/v) was added to the HMSN. The reaction was conducted for a duration of 24 hours at room temperature. The product was dialysis and freeze-dried [18].

The structure of Pluronic had two –OH groups at both ends. Following the activation of both ends with NPC, the product was further reacted with 3-amino-1-propanol to form an –OH group at one end, symbolized as NPC-F127-OH. Firstly, 5 g of F127 in a solid state was melted at 65 °C in a vacuum environment for approximately 1 hour and 30 minutes to ensure complete melting. Afterward, 0.18 g of NPC was stirred at 65 °C, under a N_2 atmosphere for a period of 5 hours. The temperature was reduced to 40 °C, 10 ml of THF was added, and the mixture was stirred at the temperature for 16 hours. A mixture of 0.03 ml of 3-amino-1-propanol and THF was added and stirred magnetically for 5 hours at room temperature. The product was obtained by precipitation by means of diethyl ether.

2.4. Synthesis of HMSN-F127

The synthesis of HMSN-F127 was conducted through the reaction between the prepared HMSN-NH_2 with NPC-F127-OH. 50 mg of HMSN-NH_2 was dispersed in 10 ml of deH_2O, thereby resulting in a solution. Concurrently, a solution of NPC-F127-OH in deH_2O was also prepared, denoted B solution. Then, solution B was added to mixture A in a gradual manner and stirred for 2 hours at a speed of 350 rpm. The obtained product was dialyzed with distilled water through a 12-14 kDa cellulose

membrane and was subsequently freeze-dried.

2.5. Characterization

The morphology and surface of the material were examined by means of scanning electron microscope (SEM) at a magnification of 7000 times, using a voltage source of 15 kV and a transmission electron microscope (TEM) at an acceleration voltage of 100 kV, performed on JEM-1400 equipment. Then, employing TEM images and utilizing ImageJ software to count the particle size, combined with Origin software, the mean particle size can be determined, thus facilitating the generation of corresponding particle size distribution chart. Moreover, the particle diameter and the zeta potential were evaluated through the dynamic light scattering method by nano ZS (SZ-100, Horiba, Kyoto, Japan), set at 37 °C and 532 nm wavelength.

The structure and space group characteristics of the material were analyzed by X-ray Diffraction (XRD). The experimental conditions were as follows: an accelerating voltage of 40 kV, current intensity of 40 mA, Cu–Kα radiation = 1.54051 Å, and a scanning angle limit from 10° to 80 °. The following procedure were conducted: the analysis of functional groups, identification of organic compounds, and study of the structure by infrared spectroscopy (Fourier transform infrared spectroscopy, FTIR) on FT-IR/NIR Frontier equipment, using the KBr pellet method. The surface area was evaluated by means of the N_2 gas adsorption-desorption method at 77 K on the Trista Micromeritics 3000 equipment. The TGA experiment (Thermal gravimetric analysis) was conducted via the TGAnalyzer (Mettler Toledo, OH, USA) under a nitrogen flow with the temperature ranging from 30 °C to 800 °C.

The identification of solutions was conducted through a qualitative-quantitative analysis by employing ultraviolet-visible absorption spectroscopy on UV-Vis 1800 equipment (Shimadzu, Japan).

2.6. Preparation of HMSN-F127/Dox and drug loading capacity

Dox was loaded into HMSN-F127 using the equilibrium dialysis method. 20 mg of HMSN-F127 was dispersed in 8 mL of deH_2O. A Dox solution of 1000 ppm was then added. Once being stirred at a temperature of 20 °C for 24 hours, the loaded particles were dialyzed against deionized water for 6 hours. The water was replaced, and was used to determine the corresponding free Dox content by UV-Vis at 570 nm. Following the removal of the excess drug, the solution inside the membrane was immediately lyophilized to evaluate its drug release ability. The carrier-drug system HMSN-F127/Dox is presented by the following symbol.

Dox loading efficiency (DLE) and loading capacity (DLC) were calculated using the equations below [19,20]:

$$\text{DLE (\%)} = \frac{\text{Amount of encapsulated drug}}{\text{Initial amount of drug for loading}} \text{ x } 100 \quad (1)$$

$$\text{DLC (\%)} = \frac{\text{Amount of encapsulated drug}}{\text{Total amount of drug and carriers}} \text{ x } 100 \quad (2)$$

2.7. In vitro release study

The release profile of the loaded HMSN-F127 was assessed in PBS buffer (0.01 M) at physiological temperature (37 °C) using the dialysis method. Firstly, the HMSN-F127/Dox drug-carrier system was dissolved in 1 ml of deH2O, and the samples were transferred to separate 6-8 KDa cellulose membranes. The dialysis membranes were immersed in a vial containing 20 mL of the release medium in PBS with pH 7.4 and 5.5, respectively. Afterwards, the content of vial was stirred at 37 °C. At predetermined times, including 1, 3, 6, 9, 12, 24, 36, 48, and 72 hours, every 2 ml of the solution outside the membrane was removed and 2 ml of buffer was added. The measurement of the absorbance of the solutions outside the membrane is to be conducted by UV-Vis spectrophotometry, after which the drug release curve of the corresponding samples is to be plotted.

2.8. Cell viability test

The assessment of cell viability was conducted through the MTT assay. The hepatocellular carcinoma cell line (HCC J5) was cultured in DMEM medium supplemented with L-glutamine (2 mM), 1.5 g/L $NaHCO_3$, penicillin (100 U/mL), streptomycin (100 µg/mL), and 10% (v/v) fetal bovine serum FBS. The cultivation was conducted at a temperature of 37 °C in a 5% CO_2 atmosphere.

On 96-well culture plates, single cells were planted at a density of 1×10^4 cells/well. Following a 24-hour culture period, the cell populations were cultured for 48 hours with varying doses of Dox, HMSN-F127, and HMSN-F127/Dox. Following the addition of 20 µl of MTT (5 mg/mL) to each well, the wells were incubated at 37 °C for a period of four hours. The culture medium was then removed, 100 µl of DMSO was added to each well, and the mixture was stirred gently for 2 minutes. The plates were then measured for absorbance at a wavelength of 570 nm. The experiments were repeated three times, and the results are presented as mean ± standard deviation.

After having the optical density value at a wavelength of 570 nm (denoted as OD570), the calculation of OD570 = ODtb – Odblank was performed followed by the calculation of the cytotoxicity rate (%) in accordance to the following formula:

$$\%\,\text{I} = \left(1 - \frac{\text{OD}_{\text{TN}}}{\text{OD}_{\text{C}}}\right) \times 100 \quad (3)$$

with:
- ODtb: OD value of the well containing cells
- ODblank: OD value of the blank well (without cells)
- ODTN: OD value of the test sample
- ODC: OD value of the control sample.

Data were calculated based on mean ± standard deviation.

3. Results and Discussion

3.1. Synthesis of HMSN-F127

The morphology and size of HMSN and HMSN-F127 particles are depicted in Fig. 1 via SEM and TEM images. It was observed that HMSN-F127 particles had a spherical shape,

which was comparable to that of the HMSN particles. Both samples exhibited a well-defined spherical morphology with a hollow interior structure, which is a typical characteristic of HMSN synthesized via the hard-template method. Similar hollow architectures have been extensively reported and are recognized for their capacity to provide a large internal cavity for drug encapsulation [21]. In addition, in contrast to the unmodified HMSN, after surface modification with F127, the SEM image of HMSN-F127 exhibited a structure characterized by a large pore inside. The diameter of HMSN was measured to be 120.8 ± 0.6 nm, while that of HMSN coated with F127 was 152.9 ± 0.9 nm. This indicates that the particle size increased by approximately 30 nm. In particular, the TEM image of HMSN-F127, stained with phosphotungstic acid solution, shows the presence of a thicker shell on the surface (Fig. 1(d)). This increase can be attributed to the formation of a polymer layer on the particle surface, which is consistent with previous studies on Pluronic-coated silica nanoparticles. In this study, size increases of 20–60 nm are commonly observed, dependent upon the concentration of F127 deposited onto the silica surface [22]. Importantly, the particle size of HMSN-F127 (152.9 ± 0.9 nm) falls within the optimal range (100–200 nm) for tumor accumulation via the enhanced permeability and retention (EPR) effect. It is well recognized that nanoparticles within this size range are capable of achieving prolonged circulation time while avoiding rapid renal clearance and uptake by the reticuloendothelial system. Consequently, the obtained size is deemed suitable for passive tumor targeting applications. [23-26]

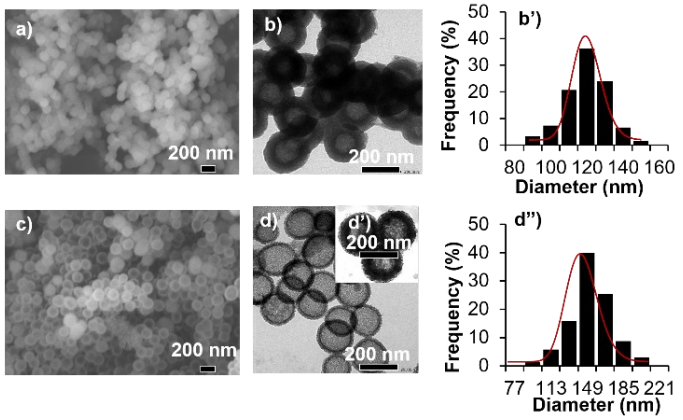

Fig. 1. SEM (a, c), TEM images (b, d) and size distribution histograms for HMSN and HMSN-F127 (b', d'), respectively

The crystal structures of HMSN-F127 were determined and compared using X-ray diffraction (see Fig. 2). The result demonstrated that the non-sharp peaks are the characteristic of the amorphous silica particles. In a previous study on the surface modification of HMSN with mPEG, the XRD spectrum of HMSN-NH2 was shown [27]. The XRD patterns of HMSN and HMSN-F127 were found to be highly similar, suggesting that the modified F127 did not impact the structure of HMSN. It was determined that no additional peaks appeared in the XRD results. It is important to note that, due to the inherently amorphous nature of silica, XRD analysis alone cannot fully resolve all structural aspects of the material. Therefore, complementary characterization techniques, including FTIR and TGA analyses, were employed to provide additional insights into the material properties and to support the successful association of F127 onto the HMSN surface.

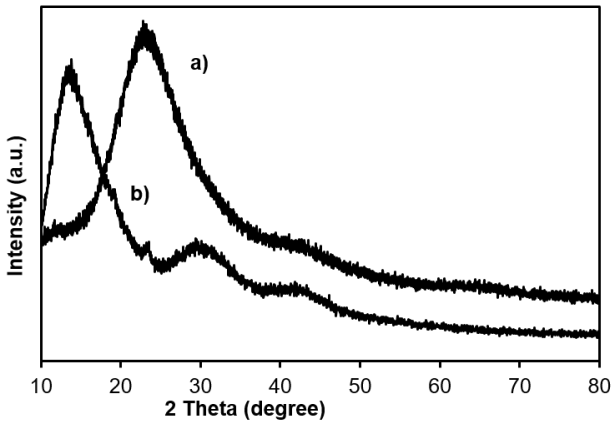

Fig. 2. Large-angle powder XRD patterns of HMSN (a), and HMSN-F127 (b)

FTIR was utilized to analyze the surface-coated HMSN particles with F127, and the results are depicted in Fig. 3. The spectra of HMSN-F127 (path a) exhibited the absorption signals of both HMSN particles by the amine group (path c) and the bare F127 (path b). The FTIR spectrum of HMSN-F127 exhibited signals at 3300 - 3500 cm^{-1} and 1089 cm^{-1}, corresponding to the -OH and Si-O-Si groups on HMSN, in addition to signals at 2888 cm^{-1} and 1111 cm^{-1}, corresponding to the $-OCH_2-CH_2-$ group on F127 [28, 29]. The results of FTIR, together with TEM images, demonstrated the successful synthesis of the HMSN-F127 particles.

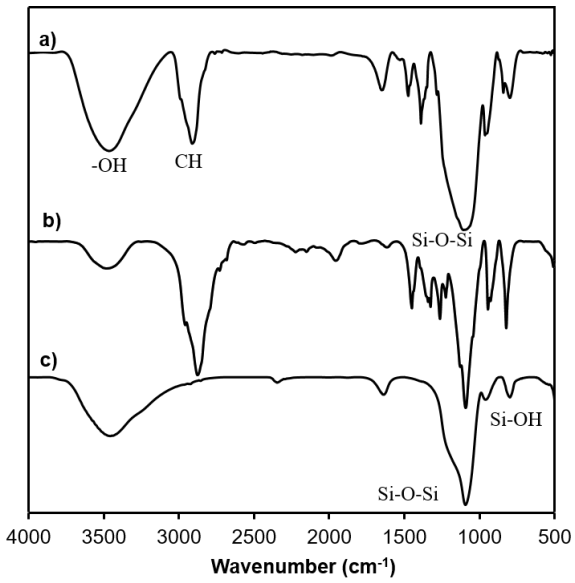

Fig. 3. FTIR spectra of HMSN-F127 (a) F127 (b), and HMSN (c)

Determining the surface properties of nanoparticle drugs is crucial as the properties influence their interactions with the environment. The environmental interaction of the drugs are dependent on the combination of size and surface properties, as well as their solubility, stability, and degree of elimination by the

body. Fig. 4 depicts the surface charges of HMSN and HMSN-F127, with zeta values of -27.5 mV and -4.03 ± 0.15 mV, respectively. The marked decrease in zeta potential after F127 association suggests effective surface charge screening by the non-ionic polymer. While the near-neutral value (−4.03 mV) indicates a degree of weak electrostatic stabilization, it does not necessarily reflect poor colloidal stability. Whilst a |zeta potential| of ~20 mV is frequently considered as a threshold for electrostatic stabilization, stable dispersions at lower values have been reported [30]. This phenomenon can be attributed to the presence of Pluronic F127, where stability is primarily governed by steric effects. The hydrated polyethylene oxide (PEO) chains form a protective layer around the nanoparticles, thereby preventing aggregation through steric hindrance. Therefore, the HMSN-F127 system is expected to maintain good dispersion stability despite its low zeta potential.

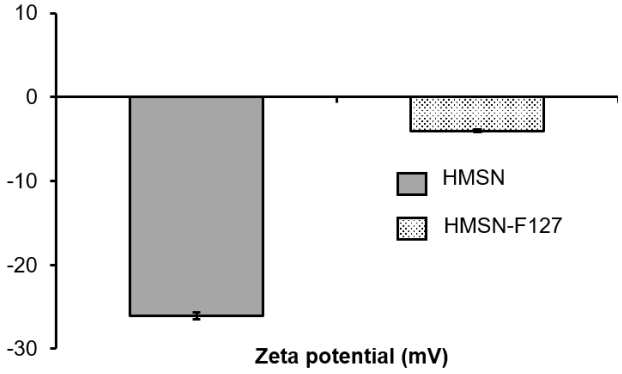

Fig. 4. Zeta potential of HMSN and HMSN-F127, respectively

The composition ratio of the constituents of the material presented in Fig. 5 was determined by means of TGA analysis. The results demonstrated that the amount of F127 coated on the surface of the hollow mesoporous silica nanoparticles was approximately 20%.

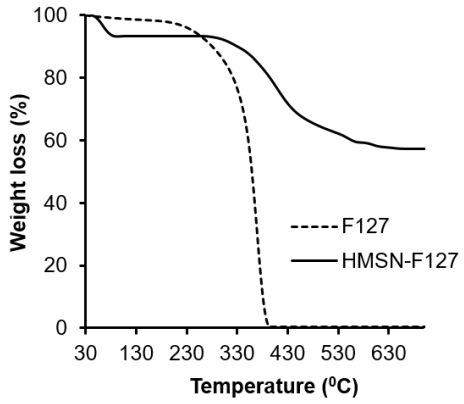

Fig. 5. Thermogravimetric analysis for HMSN-F127 (solid line) and F127 (dashed line)

As illustrated in Fig. 6, the isotherms of HMSN-F127 were identified as type IV, and the hysteresis loop was classified as H2 type according to the IUPAC classification system. The capillary condensation of HMSN-F127 at a relative pressure of 0.42 occurs early, indicating that the material has a small to medium capillary structure [31]. The surface area of HMSN-F127 was determined to be 168.4 m²/g. Thus, the F127 polymer with a molecular weight of approximately 12 kDa should have longer polymer chains on the surface of HMSN; therefore, the surface area was smaller than that of HMSN. The presence of these polymer chains may partially cover the mesopore openings and hinder nitrogen diffusion into the pore channels during BET analysis. Consequently, it can lead to reduced accessible surface area. Similar reductions have been widely reported in polymer-coated mesoporous silica systems due to pore blocking and steric hindrance effects [32]. Importantly, the retention of the type IV isotherm and H2 hysteresis loop confirms that the mesoporous structure is still well preserved after modification. Therefore, the decrease in surface area is considered to be a consequence of successful incorporation of F127, rather than structural collapse. This is consistent with the findings of previous research on F127-functionalized HMSN materials.

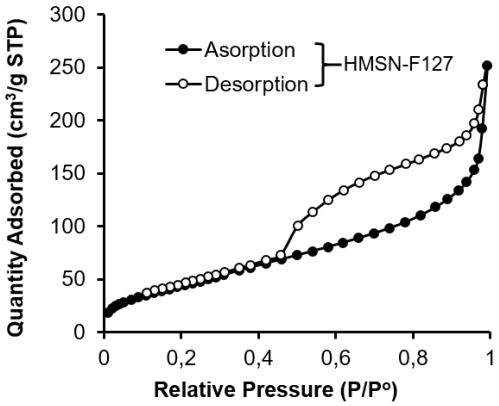

Fig. 6. N_2 adsorption-desorption isotherm of HMSN-F127

In any drug delivery system, drug loading efficiency and drug carrying content are considered as two crucial factors as they play a direct role in determining the therapeutic activity [33]. In particular, HMSN has been approved for biomedical applications by the FDA. Following conjugation with F127, the DLE and DLE of HMSN-F127 were found to be higher than those of naked HMSN. The values obtained were 72.08 ± 0.09% and 11.09 ± 0.01%, respectively. This result is comparable to or higher than many previously reported HMSN-based systems. For example, conventional HMSN typically exhibit loading efficiencies of approximately 50–60% [34], while functionalized mesoporous silica systems frequently demonstrate moderate drug loading depending upon surface chemistry and interaction with Dox [35]. In certain optimized systems, high loading efficiency can be achieved due to strong electrostatic interactions, particularly for charged drugs such as Dox [36].

For these carrier systems, the amount of drug was not only contained in the structure of the HMSN particles but also in the slots formed by the polymers on the surface. These polymers acted as covers to limit drug leakage during transportation, thereby leading to a higher drug carrying capacity. Furthermore, F127 is a thermosensitive polymer; consequently, the drug encapsulation process was carried out at low temperatures (20 °C). At this temperature, the F127 polymers undergo a

stretching process, enabling the drug to be readily inserted into the pores through the utilization of magnetic stirring. As the temperature increased (≥ 25°C), these polymers clustered to hold the drug within the structure and on the polymer surfaces. This, in turn, resulted in an enhancement of the drug-carrying capacity of the HMSN-F127 carrier system.

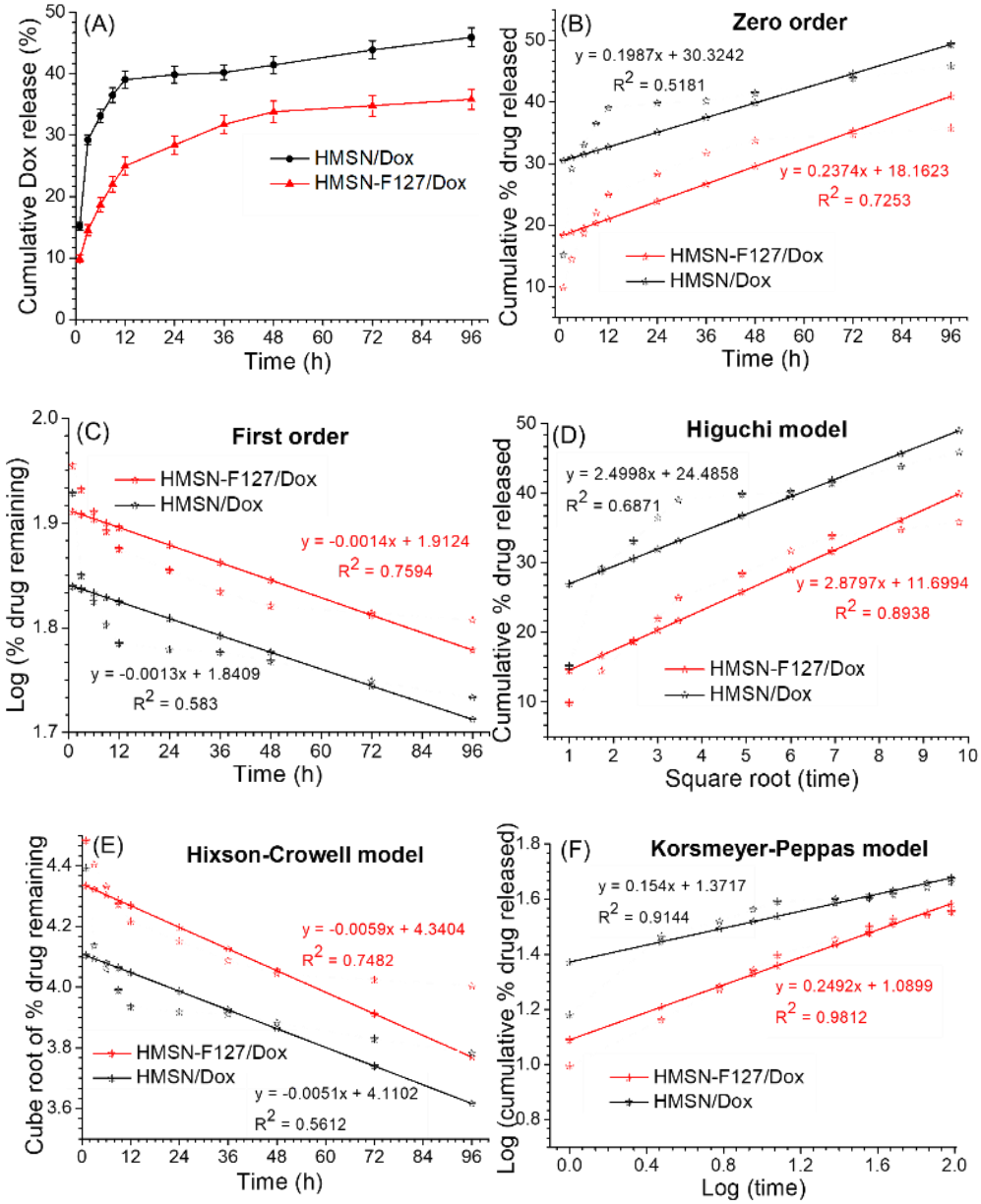

Fig. 7. *In vitro* release and kinetic analysis of Dox from HMSN and HMSN-F127 nanoparticles. (a) Cumulative Dox release profiles from HMSN/Dox and HMSN-F127/Dox at pH 5.5. (b) Dox release fitted to kinetic models: zero-order, (c) first-order, (d) Higuchi, (e) Hixson–Crowell, (f) and Korsmeyer–Peppas

Fig. 7 depicts the evaluation of the drug release ability of the HMSN-F127/Dox drug delivery system. The results demonstrated that HMSN-F127/Dox exhibited a slower and more sustained release profile in comparison to HMSN/Dox at a pH of 5.5 (Fig. 7(a)). The initial release of HMSN was relatively rapid, reaching 39.03% at 12 hours and gradually increasing to 45.91% at 96 hours. In contrast, HMSN-F127/Dox released only 24.95% at 12 hours and reached a lower cumulative release of 35.81% at 96 hours, indicating a clear retardation effect after F127 association. The release behavior can be divided into two stages. The initial phase (0–12 hours) is characterized by a accelerated release, attributed to the diffusion of Dox molecules located in close to or on the particle surface. This is followed by a slower and sustained release phase (12–96 h), governed by the diffusion of Dox from the internal mesoporous structure. The reduced release rate observed for HMSN-F127/Dox can be explained by the presence of the F127 polymer layer, which acts as a diffusional barrier. The hydrated polymer chains have been shown to partially restrict solvent penetration and drug transport, thereby suppressing the burst release and promoting a more controlled release profile.

The release kinetics of Dox from HMSN and HMSN-F127 were systematically analyzed using various kinetic models (see Table 1 and Fig. 7(b–f)) to elucidate the underlying release

mechanism. The zero-order model demonstrated suboptimal fitting for both systems ($R^2 < 0.73$), indicating that Dox release does not proceed at a constant rate. Similarly, the first-order model exhibited only moderate correlation (R^2 = 0.58–0.76), suggesting that drug release is partially concentration-dependent, particularly during the initial stage. In contrast, the Higuchi model provided a better fit, particularly for HMSN-F127 (R^2 = 0.8938) in comparison to HMSN (R^2 = 0.6871), indicating that diffusion through the mesoporous matrix plays a dominant role on the regulation of drug release. This trend is further supported by the Korsmeyer–Peppas model, which exhibited the highest correlation coefficients (R^2 = 0.9144 for HMSN and 0.9812 for HMSN-F127). The corresponding release exponent values (n = 0.154 and 0.2492, respectively) are both below 0.45, thus confirming a Fickian diffusion mechanism. The results obtained demonstrate that the release of Dox is primarily governed by concentration-driven diffusion from the mesoporous structure. The slightly higher R^2 value for HMSN-F127 suggests a more consistent diffusion-controlled process, likely due to the presence of the F127 layer acting as an additional diffusional barrier. The release profile follows a biphasic pattern, consisting of an initial burst release of surface-associated drug, followed by a sustained diffusion phase from the pores. The incorporation of F127 does not alter the fundamental release mechanism; rather, it effectively modulates the diffusion rate, thereby leading to enhanced release control.

As demonstrated in previous publications, the biocompatibility of nanoporous silica and F127 polymers has been shown to make them suitable for drug delivery. However, the modification of these polymers on the surface of HMSN particles in the study used organic solvents. Consequently, the toxicity of the carrier system was evaluated based on the cytotoxic activity test on HCC J5 liver cancer cells, as shown in Fig. 8 and Fig. 9. Fig. 8(a) demonstrates that after 48 hours at concentrations from 0 to 250 µg/ml, with cell viability remained above 85% even at the highest concentration. This result confirms the excellent cytocompatibility of the carrier system and indicates that the surface modification with F127 does not induce significant toxicity to the HCC J5 cells. At a concentration of 10 µg/mL, our previous studies have reported a near-complete loss of cell viability in HCC J5 cells, indicating the strong anticancer activity of Dox under similar experimental conditions [18]. In particular, when Dox was encapsulated in HMSN-F127/Dox nanocarriers, its toxicity was reduced in comparison to the control Dox (Fig. 8(b)). The results demonstrate that the cytotoxicity of HMSN-F127/Dox is lower than that of free Dox at equivalent concentrations. This phenomenon can be attributed to the sustained and controlled release behavior of the nanocarrier system. The presence of the F127 layer and mesoporous structure likely modulates drug diffusion, resulting in slower intracellular accumulation of Dox and a more gradual cytotoxic response. Furthermore, the morphological observations in Fig. 9 corroborate the quantitative cell viability results. As the concentration of Dox increases, HCC J5 cells exhibit progressive structural changes, including cell shrinkage, reduced cell density, and loss of adhesion. These features are indicative of the cytotoxic effects induced by chemotherapeutic agents.

Table 1. Kinetic modeling parameters and fitting coefficients for Dox release from HMSN-F127/Dox and HMSN/Dox formulations

Model	Parameters at pH 5.5	Dox formulation	
		HMSN-F127/Dox	HMSN/Dox
Zero-order model $Q_t/Q_\infty = K_0t + C_0$	K_0	0.2374	0.1987
	C_0	18.1623	30.3242
	r^2	0.7253	0.5181
First-order model $\ln(1-Q_t/Q_\infty) = K_1t + C_1$	K_1	-0.0014	-0.0013
	C_1	1.9124	1.8409
	r^2	0.7594	0.5830
Higuchi model $Q_t/Q_\infty = K_Ht^{0.5} + C_H$	K_H	2.8797	2.4998
	C_H	11.6994	24.4858
	r^2	0.8938	0.6871
Hixson –Crowell mode $(1- Q_t/Q_\infty)^{1/3} = K_{HC}t + C_{HC}$	K_{HC}	-0.0059	-0.0051
	C_{HC}	4.3404	4.1102
	r^2	0.7482	0.5612
Korsmeyer-Peppas $Q_t = K_{KP}t^n$	K_{KP}	0.1230	0.2353
	n	0.2492	0.1540
	r^2	0.9812	0.9144
	Order of release	Fickian	Fickian

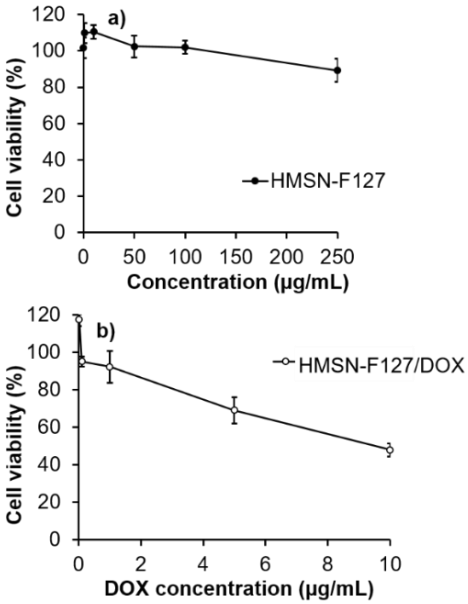

Fig. 8. Cytotoxicity curves on HCC J5 cell line of (a) HMSN-F127 and (b) HMSN-F127/Dox

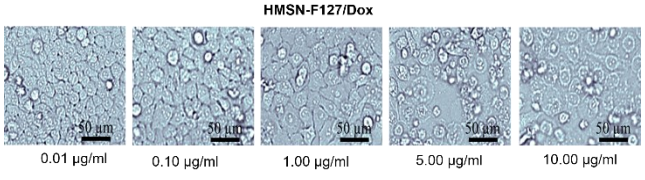

Fig. 9. HCC J5 cells treated by HMSN-F127/Dox at different Dox concentrations in MTT assays

4. Conclusion

The development of HMSN-F127 nanocarriers has been demonstrated to yield enhanced performance in comparison to bare HMSN. F127 incorporation resulted in an increase in particle size (120.8 ± 0.6 to 152.9 ± 0.9 nm) and a shift in zeta potential from −27.5 to −4.03 mV, confirming effective surface association. This modification led to a reduction in burst release (from 39.03% to 24.95% at 12 hours) and a decrease in cumulative release (from 45.91% to 35.81% at 96 hours), indicating enhanced control over drug diffusion. HMSN-F127 exhibited good cytocompatibility with viability levels exceeding 85% while preserving the dose-dependent anticancer activity of Dox. The results demonstrate that F127 functionalization effectively regulates drug release and highlights the potential of HMSN-F127 as a platform for controlled drug delivery.

Acknowledgement

We acknowledge the support of time and facilities from Tra Vinh University (TVU) for this study.

We acknowledge the support of time and facilities from Institute of Advanced Technology – Vietnam Academy of Science and Technology for this study.

References

1. Chen, F., et al., *Engineering of hollow mesoporous silica nanoparticles for remarkably enhanced tumor active targeting efficacy*, Scientific reports. 4 (2014) 5080.
2. Wu, S., X. Huang, and X. Du, *pH-and redox-triggered synergistic controlled release of a ZnO-gated hollow mesoporous silica drug delivery system*, Journal of Materials Chemistry B. 3 (2015) 1426-1432.
3. Cotí, K.K., et al., *Mechanised nanoparticles for drug delivery*, Nanoscale. 1 (2009) 16-39.
4. Yang, L. and P. Alexandridis, *Physicochemical aspects of drug delivery and release from polymer-based colloids*, Current opinion in colloid & interface science. 5 (2000). **5**(1-2) 132-143.
5. Russo, E. and C. Villa, *Poloxamer Hydrogels for Biomedical Applications*, Pharmaceutics. 11(2019) 671.
6. Ruel-Gariepy, E. and J.-C. Leroux, *In situ-forming hydrogels—review of temperature-sensitive systems*, European Journal of Pharmaceutics and Biopharmaceutics. 58 (2004) 409-426.
7. Teotia, A., H. Sami, and A. Kumar, *Thermo-responsive polymers: structure and design of smart materials*, in Switchable and responsive surfaces and materials for biomedical applications. (2015) 3-43.
8. Zhang, W., et al., *Synthesis and characterization of thermally responsive pluronic F127− chitosan nanocapsules for controlled release and intracellular delivery of small molecules*, ACS nano. 4 (2010) 6747-6759.
9. Zeng, Z., et al., *Facile fabrication of thermally responsive Pluronic F127-based nanocapsules for controlled release of doxorubicin hydrochloride*, Colloid and Polymer Science. 292 (2014) 1521-1530.
10. Nguyen, T.T.C., et al., *Highly lipophilic pluronics-conjugated polyamidoamine dendrimer nanocarriers as potential delivery system for hydrophobic drugs*, Materials Science and Engineering: C. 70 (2017) 992-999.
11. Kim, J.D., et al., *Thermo-responsive human α-elastin self-assembled nanoparticles for protein delivery*, Colloids and Surfaces B: Biointerfaces. 149 (2017) 122-129.
12. Zhao, D., et al., *Triblock copolymer syntheses of mesoporous silica with periodic 50 to 300 angstrom pores*, Science. 279 *(*1998) 548-552.
13. Liu, Z., J. Ding, and J.J.N.J.o.C. Xue, *A new family of biocompatible and stable magnetic nanoparticles: silica cross-linked pluronic F127 micelles loaded with iron oxides*, New Journal of Chemistry. 33 *(*2009) 88-92.
14. Organization, W.H., *WHO model list of essential medicines: 17th list*, March 2011. (2011).
15. Tacar, O., P. Sriamornsak, and C.R. Dass*, Doxorubicin: an update on anticancer molecular action, toxicity and novel drug delivery systems,* Journal of pharmacy and pharmacology. 65 (2013) 157-170.
16. Mobaraki, M., et al., *Molecular mechanisms of cardiotoxicity: a review on major side-effect of doxorubicin*, Indian Journal of Pharmaceutical Sciences. 79 (2017) 335-344.
17. Nguyen-Thi, N.-T., et al., *The engineering of porous silica and hollow silica nanoparticles to enhance drug-loading capacity*, Processes. 7 (2019) 805.
18. Nguyen, T.N.T., et al., *Aminated hollow mesoporous silica nanoparticles as an enhanced loading and sustained releasing carrier for doxorubicin delivery*, Microporous and Mesoporous Materials. 309 (2020) 110543.
19. Liu, J., et al., *Hollow mesoporous silica nanoparticles facilitated drug delivery via cascade pH stimuli in tumor microenvironment for tumor therapy*, Biomaterials. 83 (2016) 51-65.
20. Chen, Y., et al., *Hollow/rattle-type mesoporous nanostructures by a structural difference-based selective etching strategy*, ACS nano. 4 (2009) 529-539.
21. Slowing, I.I., et al., *Mesoporous silica nanoparticles as controlled release drug delivery and gene transfection carriers*, Advanced drug delivery reviews. 60 *(*2008) 1278-1288.
22. Carbone, C., et al., *Adsorption of Mixed Dispersions of Silica Nanoparticles and an Amphiphilic Triblock Copolymer at the Water–Vapor Interface*, Applied Sciences. 13 (2023) 10093.
23. Peer, D., et al., *Nanocarriers as an emerging platform for cancer therapy*, Nano-enabled medical applications. (2020) 61-91.
24. Nguyen, N.T., et al., *Development and Characterization of Folic Acid-Decorated Fucoidan-Poloxamer 407 Self-Assembled Nanogels Co-Loading Curcumin and Paclitaxel for Synergistically Enhanced Chemotherapeutic Efficacy*, Journal of Polymer Science. 63 (2025) 2405-2421.
25. Nguyen, N.T., et al., *Efficient and controllable co-delivery of paclitaxel and curcumin from fucoidan-pluronic F127 nanogel for synergistic breast cancer treatment*, Macromolecular. 32 (2024) 427-442.
26. Ly, H.Q., et al., *Optimization of the poloxamer 407-conjugated gelatin to synthesize pH-sensitive nanocarriers for controlled paclitaxel delivery*, Journal of Polymer Research 32 (2025) 38.
27. Nguyen, T.N.T., et al., *Surface PEGylation of hollow mesoporous silica nanoparticles via aminated intermediate*, Progress in Natural Science: Materials International. 29 (2019) 612-616.
28. Peer, D., et al., *Nanocarriers as an emerging platform for cancer therapy,* Nature nanotechnology. 2 (2007) 751-760.
29. Davis, M.E., Z. Chen, and D.M. Shin, *Nanoparticle therapeutics: an emerging treatment modality for cancer*, Nature reviews Drug discoveryjournals. 7 (2008) 771-782.
30. Cortés, H., et al., *Non-ionic surfactants for stabilization of polymeric nanoparticles for biomedical uses,* Materials. 14 (2021) 3197.
31. Sing, K.S., *Reporting physisorption data for gas/solid systems with special reference to the determination of surface area and porosity (Recommendations 1984)*, Pure and applied chemistry. 57 (1985) 603-619.

32. Xing, L., et al., *Coordination polymer coated mesoporous silica nanoparticles for pH-responsive drug release*, Advanced Materials (Deerfileld Beach, Fla.). 24 (2012) 6433-6437.
33. Shen, S., et al., *High drug-loading nanomedicines: progress, current status, and prospects*, International journal of nanomedicine. 12 (2017) 4085.
34. Nguyen-Thi, N.-T., et al., *The engineering of porous silica and hollow silica nanoparticles to enhance drug-loading capacity*, Processes. 7 (2019) 805.
35. Day, C.M., et al., *Functionalized mesoporous silica nanoparticles as delivery systems for doxorubicin: drug loading and release*, Applied Sciences. 11 (2021) 6121.
36. Guo, L., et al., *A comprehensive study of drug loading in hollow mesoporous silica nanoparticles: Impacting factors and loading efficiency*, Nanomaterials. 11 (2021) 1293.